PHYSICAL REVIEW A VOLUME 24, NUMBER 3 SEPTEMBER 1981

Ionization of one-electron ions and capture by bare and one-electron ions of C, N, O, and F on He

T. R. Dillingham, J. R. Macdonald, and Patrick Richard
J. R. Macdonald Laboratory, Kansas State University, Manhattan, Kansas 66506
(Received 4 February 1981)

Experimentally measured single-electron-transfer cross sections are presented for bare nuclei and one-electron ions of C, N, O, and F following collisions with a He-gas target in the energy range from ~0.5–2.5 MeV/amu. Excellent agreement is found between the K-shell ionization cross sections (electron loss by one-electron ions) and a theoretical plane-wave–Born-approximation calculation without inclusion of Coulomb-deflection and binding-energy corrections. Comparisons are also made between the capture cross sections (electron gain) and previously measured total projectile x-ray cross sections. The ratio of the x-ray cross section to the total capture cross section is compared to the same ratio found through a Brinkman-Kramers (BK) calculation. The results of the comparison show that the single normalization constant for the capture to each state, which was used in the theoretical analysis of the x-ray cross section, is inadequate. In particular, the results show that the BK calculation underestimates the capture of the electron to the 1s and 2s states as compared to the higher, x-ray-emitting states. The total capture cross sections are also given as a function of E/M (MeV/amu). For a given velocity the capture is dependent only upon the charge state of the incident ion. Also, the similar velocity dependence with average ratios of 1:0.68:0.44 for the charge-changing processes $q \rightarrow q-1$ ($q = 8$, 7, and 6) correspond to a q^3 dependence for the total cross section.

I. INTRODUCTION

The processes that can occur in an ion-atom collision define a subject which has aroused a great deal of interest over the past years.[1] Renewed interest in understanding these processes stems from their applications to such diverse fields of study as fusion technology[2] and x-ray astronomy.[3] In addition, the subject is of considerable theoretical interest.[4] By utilizing the well-known Coulomb potential and the known initial and final atomic states, one hopes to be able to test the validity of various approximations to collision theory.

There are many commonly identified processes that can take place with various degrees of probability when an incoming projectile interacts inelastically with a target atom. Some of these include the capture of one or more electrons from the target by the projectile, ionization of the projectile electrons (electron loss), ionization of the target electrons, and excitation of either or both the projectile and target atoms. Often, the reactants are left in excited states following the collision and photons or electrons may be emitted, either independent of the collision or perturbed by it, and observation of these has led to much of our knowledge of the collision mechanisms.[1] Although all the processes are of current interest, this paper will be limited to the study of the single-electron processes in which one electron is captured by a bare or one-electron projectile ion or lost by an initial ground-state one-electron projectile ion interacting with helium target atoms. The experimental techniques used are similar to those used in previous studies[5,6] of charge exchange by the "initial growth method," performed for various ions over a range of energies. Review of earlier work has been given by Allison and Garcia-Munoz,[7] Nikolaev,[8] Betz,[9] and Tawara and Russek.[10] Other than for low-Z projectiles (H and He) there has been no concerted effort to study these processes for the well-defined initial states of a one-electron ion for which theoretical calculations are presumably possible.

One of the prime purposes of the present work is to use projectile charge-change measurements to determine K-shell ionization cross sections which have previously been determined from other types of experiments,[11] for example, x-ray or Auger electron measurements. The latter work has focused on ionization of inner-shell electrons from neutral target atoms while the present work is limited to the ionization of hydrogenlike projectile ions in collision with simple atoms, i.e., He. The understanding of the process of ionization of neutral atoms by collision with a charged particle is complicated by the presence of other electrons on the atoms.[12] For the one-electron ions used in this experiment, the wave functions are purely hydrogenic (unscreened) and no screening parametrization is required for the electron to be ionized.

In most previous experimental work dealing with the ionization process, it has been tacitly assumed that target atoms are ionized by swift, point charge, projectiles. In recent work by Tawara *et al.*[13] the charge state dependences of single K-shell electron excitation and single K-shell ionization of the projectile were studied for F^{q+} + He

 © 1981 The American Physical Society

collisions by high-resolution x-ray spectroscopy. It was shown that the excitation cross section increased and the ionization cross section decreased with increasing charge state of the projectile. This method can be used to study excitation of one-electron projectiles but cannot be used to study ionization of one-electron projectiles since there is no x-ray emission. In this work, ionization of the one-electron projectile ion is studied. The comparison with other work is straightforward since it is the relative velocity between the projectile and target which defines the collision, and not which atom is the projectile. However, we must examine the role of target electrons which are present on the neutral target atom. The present experimental results must be compared at the same relative velocity, not laboratory energy, to calculations and other relevant measurements. Cross sections are defined with the relative velocity as an important parameter.

One complication to the interpretation of the present experiment, not present in more traditional work, is the presence of outer-shell electrons on the helium target atoms interacting with the projectiles. The consequence of the screening of these electrons has not been well established in the literature and remains a subject for further investigation.[14,15]

II. EXPERIMENTAL

To perform this experiment, ions of carbon, nitrogen, oxygen, and fluorine were extracted from the Kansas State University tandem Van de Graaff accelerator. The ions were momentum analyzed by a 90° analyzing magnet and passed through a thin carbon foil (5–20 $\mu g/cm^2$) to produce a distribution of charge states. The charge state of interest was then selected by a switching magnet which directed the beam down the beam line to the target chamber. This technique provided ions of a range of charge states at the same beam energy. The target chamber consisted of a differentially pumped gas cell defined by four optically aligned circular apertures. The overall length of the gas cell was 19.61 cm. The pumping of the cell was accomplished by means of a 4-inch oil diffusion pump connected directly in front of and behind the gas cell. Two other diffusion pumps were also utilized to maintain a residual gas pressure of 10^{-6} to 10^{-7} Torr in the beam line. Maintaining a constant pressure within the target chamber was accomplished by means of a Granville-Phillips automatic pressure controller. The pressure was monitored by an MKS baratron capacitance manometer which sent a signal to the pressure controller (to open or close a servo-driven leak valve to the chamber) whenever the pressure deviated from a preset valve. To prevent contaminants in the He gas handling system from entering the target chamber, a liquid nitrogen trap was placed in the gas line to extract any condensable vapor contaminants within the system.

As the beam passes through the gas cell, a fraction of the incident particles undergo charge exchange with the target gas. At approximately 80 cm behind the target cell, an electromagnet was set up to spatially separate the various charge states of the emerging beam. After separating the charge states, a position-sensitive surface barrier detector was used to detect the ions of the emerging beam. The detector, supplied by Nuclear Diodes, was a silicon surface barrier detector capable of providing information about both the energy and position of the incident ion, simultaneously. When an ion enters the detector, two signals are produced. The first is the collection of all the negative charge to a low-resistance gold layer on the front of the detector and gives a signal proportional to the total energy of the incident particle. The second is from the collection of a portion of the positive charge collected on a resistive strip in the back of the detector. This signal is the product of the energy of the particle times the fraction of the length from the grounded end of the resistive layer and hence represents the position at which the ion impacted. Since the various charge states are spatially separated by the electromagnet, the position-sensitive detector was used to determine the relative number of ions in a given state of the emerging beam. Background particles, which have different energy but the same magnetic rigidity as the particles of interest, are prevented from being counted in the spectra by gating the position signal with the energy signal.

To perform this experiment, the counting rate of the detector was kept below 1000 cts/sec to prevent electronic pileup in the system and also to ensure a reasonable lifetime of the detector. Usually 10^5 ions were counted for each gas pressure and incident particle energy. For each energy, data for at least four different gas pressures were taken. The pressures within the target cell were chosen judiciously to ensure that the corrections to the first-order approximation in the analysis of the cross sections, and hence, the multiple processes, were in all cases small. Generally, the incident charge state was greater than 95% after undergoing charge exchange. The spectra were analyzed by integrating the number of counts in each peak and calculating the fraction of ions emerging in each charge state at the pressure of the run. The relative charge fractions

were then plotted as a function of target pressure. An example of the pressure dependence of the relative charge fractions is shown in Fig. 1 for 16-MeV O^{7+} on He. The single-electron-capture and electron-loss cross sections were then extracted by the method described in the next section.

III. ANALYSIS

In general, the change in charge state of a beam of ions as it passes through a target is given by the set of differential equations [5]

$$\frac{d\phi_i}{dx} = \sum_{j\neq i} (\sigma_{ji}\phi_j - \sigma_{ij}\phi_i) , \tag{1}$$

where ϕ_i is the fraction of ions in charge state i, x is the target thickness in atoms/cm^2, and σ_{ij} is the cross section for an ion changing from a charge state i to a state j after undergoing a collision with a target atom. Total charge-transfer cross sections are summations over cross sections for formation of well-defined atomic states and, in general, depend upon many factors including the possible distribution of final states of both projectile and target. In this work, however, attempts have been made to identify the dependence of the total charge-transfer cross sections on the relative velocity between the projectile and target, the charge state and atomic number of the incident ions, and the state of excitation of the incoming beam. Dependence upon the latter was removed by choosing a long flight path of the incident beam before it reaches the target chamber, such that the time of flight is much longer than the lifetimes of the excited states. Exceptions to this are the heliumlike $1s2s\ ^3S_1$ and the hydrogenlike $2s$ states.

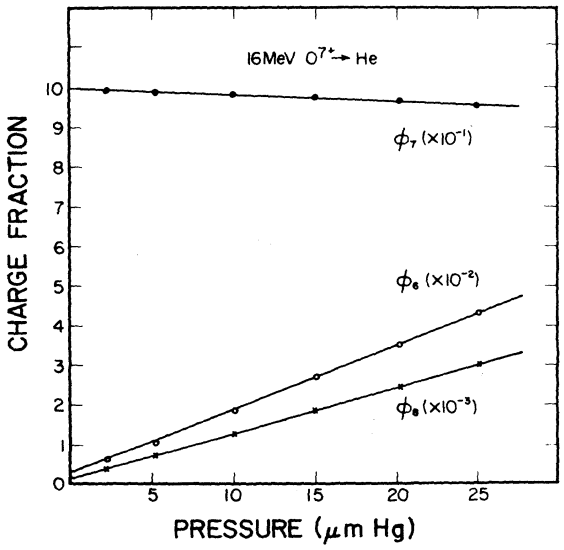

FIG. 1. The various charge fractions ϕ_i as a function of the target cell pressure in micrometers, for 16-MeV $O^{7+} \rightarrow$ He. The solid lines are drawn to guide the eye.

As a first approximation to the solution of Eq. (1), one neglects terms other than first order in target thickness x and the solution becomes

$$\phi_i = \phi_i(0) + \sum_{j\neq i} \sigma_{ji}x , \tag{2}$$

with the initial conditions $\phi_\alpha(0) \approx 1$, where α is the incident charge state, and $\phi_{i\neq\alpha} \ll 1$. Ignoring multiple processes, the single-electron-transfer cross section can be written as

$$\sigma_{\alpha i} = \frac{d\phi_i}{dx} . \tag{3}$$

Thus the slope of the charge fraction ϕ_i versus the target thickness gives a first-order approximation to the single-electron-capture and -loss cross sections. To evaluate the contribution of second-order terms to the cross section, we consider only a three-state system αij. For a helium target this is sufficient since double-electron-transfer cross sections are small. The second-order solution can be found from the equation $d\phi_i/dx = \sigma_{\alpha i}\phi_\alpha - \sigma_{i\alpha}\phi_i$ by using the first-order solutions $\phi_i = \sigma_{\alpha i}x$ and $\phi_\alpha = 1 - (\sigma_{\alpha i} + \sigma_{\alpha j})x$. The second-order solution is then given by

$$\sigma_{\alpha i} = \frac{\frac{d\phi_i}{dx}}{1 - (\sigma_{\alpha i} + \sigma_{\alpha j} + \sigma_{i\alpha})x} . \tag{4}$$

With the further approximation that $\sigma_{i\alpha} \approx \sigma_{\alpha j}$, and using the first-order solutions for the cross sections, the expression, in terms of experimental quantities, becomes

$$\sigma_{\alpha i} = \frac{\frac{d\phi_i}{dx}}{1 - \left(\frac{d\phi_i}{dx} + 2\frac{d\phi_j}{dx}\right)x} . \tag{5}$$

In general, the second-order corrections were small, usually less than 3%, although in a few instances, the corrections reached 13%.

The target thickness, x in atoms/cm^2, was related to the target cell pressure by means of the ideal-gas law. The first-order single-charge-transfer cross sections are then given by

$$\sigma_{\alpha i} = K\frac{d\phi_i}{dP(\mu)} , \tag{6}$$

where $K = RT/N_a l$ is a constant, and $R = 8.313$ J/mol K (universal gas constant), T is the temperature in K, $N_a = 6.023 \times 10^{23}$ atoms/mol, and l is the target cell length in cm. The value of K can be

found by precisely measuring (including cell end effects) the target length l. The absolute scale calibration, determined in this way, was also checked by a normalization process. To obtain the experimental cross sections, the values of $d\phi_i/dP(\mu)$ were determined for each charge fraction from the best straight-line fit to the experimental data points by a least-squares method. The slope of this line, along with the constant K, were used to find the single-charge-transfer cross sections to first order. This value was then improved by incorporating the second-order correction term given previously. This procedure was performed for each ion to obtain the single-charge-transfer cross sections over the energy range of interest.

The constant K was found by carefully evaluating the target cell length including cell end effects. The value of K measured in this fashion was found to be $K = (1.55 \pm 0.09) \times 10^{-15}$ cm^2 μm/atom. This value was checked by comparison with other experimental measurements,[5,6] which together give the charge-transfer cross sections for C, N, O, and F in argon gas. With the experimental setup and procedure used in this work, the experiments in argon were redone to obtain values for the change in the charge fraction versus pressure, $d\phi_i/dP(\mu)$. The normalization constant was then obtained by using the cross sections from the previous measurements in argon. This was done using different ions over a range of energies and the results were compared to those found through geometric considerations. The results of this comparison agree to within 6%.

An approximate normalization to experimental results is available for the electron-capture cross sections using the total x-ray cross sections for fluorine on helium by Guffey.[16] The x-ray cross sections provide a lower limit to the total electron-capture cross sections, and were used to determine a lower limit to the normalization constant. The value of the constant obtained was approximately 80% of that found geometrically. One would expect this difference since a K x ray is emitted when the electron is captured to a state other than the 1s and 2s states and then only with a branching ratio that is approximately 88%.[16] Hence, the total x-ray cross section is less than the total capture cross section and the results of this comparison confirm the magnitude of the x-ray cross sections to an accuracy of approximately 30%.

For the normalization of the final data, the value used for the normalization constant K was the value found through geometric considerations [$K = (1.55 \pm 0.09) \times 10^{-15}$ cm^2 μm/atom]. The other methods used, namely, comparisons with previous measurements in argon and x-ray measurements, confirm the choice of this constant to within the experimental error.

IV. RESULTS AND DISCUSSION

A. Experimental cross sections

Single-electron-capture and electron-loss cross sections were measured as a function of energy for bare nuclei and one-electron ions of carbon, nitrogen, oxygen, and fluorine incident on helium gas. The cross sections were extracted by the "initial growth method" and the results of these measurements and their uncertainties are given in Tables I–IV. The results can also be seen in graphical form in Fig. 2 where the cross sections are plotted as a function of incident ion energy. The solid lines in the figure are drawn to guide the eye.

In general, the single-electron-capture cross sections fall off by several orders of magnitude over the energy range of interest for the various incident ions used. The single-electron loss or K-shell ionization cross sections exhibit a very broad maximum over the energy range of this work, that is, near the peak of the cross section.

TABLE I. $C^{q+} \rightarrow$ He; cross sections σ_{ij} in cm^2/atom with relative uncertainties.

Energy (MeV)	σ_{65}	σ_{54}	σ_{56}
6.03	$(2.49 \pm 0.15) \times 10^{-17}$	$(1.36 \pm 0.07) \times 10^{-17}$	$(5.07 \pm 0.52) \times 10^{-19}$
8.33	$(7.78 \pm 0.65) \times 10^{-18}$	$(4.01 \pm 0.28) \times 10^{-18}$	$(6.60 \pm 0.67) \times 10^{-19}$
10.5	$(2.87 \pm 0.14) \times 10^{-18}$	$(1.42 \pm 0.07) \times 10^{-18}$	$(6.10 \pm 0.32) \times 10^{-19}$
12.0	$(1.77 \pm 0.17) \times 10^{-18}$	$(8.68 \pm 0.37) \times 10^{-19}$	$(7.23 \pm 0.48) \times 10^{-19}$
13.58	$(8.13 \pm 0.46) \times 10^{-19}$	$(3.61 \pm 0.22) \times 10^{-19}$	$(8.23 \pm 0.44) \times 10^{-19}$
16.0	$(5.72 \pm 0.39) \times 10^{-19}$	$(2.62 \pm 0.18) \times 10^{-19}$	$(7.78 \pm 0.35) \times 10^{-19}$
18.5	$(2.87 \pm 0.18) \times 10^{-19}$	$(1.41 \pm 0.09) \times 10^{-19}$	$(6.71 \pm 0.24) \times 10^{-19}$
18.75	$(2.81 \pm 0.27) \times 10^{-19}$	$(1.34 \pm 0.09) \times 10^{-19}$	$(6.83 \pm 0.35) \times 10^{-19}$
20.5	$(2.08 \pm 0.15) \times 10^{-19}$	$(9.12 \pm 0.54) \times 10^{-20}$	$(6.52 \pm 0.22) \times 10^{-19}$
22.5	$(1.28 \pm 0.13) \times 10^{-19}$	$(6.43 \pm 0.50) \times 10^{-20}$	$(6.24 \pm 0.22) \times 10^{-19}$
24.12	$(1.08 \pm 0.09) \times 10^{-19}$	$(4.61 \pm 0.46) \times 10^{-20}$	$(6.49 \pm 0.33) \times 10^{-19}$
25.5	$(8.39 \pm 0.75) \times 10^{-20}$	$(3.36 \pm 0.46) \times 10^{-20}$	$(6.00 \pm 0.18) \times 10^{-19}$

TABLE II. $N^{q+} \rightarrow He$; cross sections σ_{ij} in cm^2/atom with relative uncertainties.

Energy (MeV)	σ_{76}	σ_{65}	σ_{67}
5.17	$(8.22 \pm 0.95) \times 10^{-17}$	$(5.21 \pm 0.34) \times 10^{-17}$	
7.14	$(3.74 \pm 0.21) \times 10^{-17}$	$(2.20 \pm 0.08) \times 10^{-17}$	$(2.16 \pm 0.40) \times 10^{-19}$
11.64	$(5.20 \pm 0.29) \times 10^{-18}$	$(3.41 \pm 0.12) \times 10^{-18}$	$(3.71 \pm 0.32) \times 10^{-19}$
14.0	$(2.54 \pm 0.10) \times 10^{-18}$		
16.1	$(1.44 \pm 0.07) \times 10^{-18}$	$(7.67 \pm 0.33) \times 10^{-19}$	$(4.03 \pm 0.29) \times 10^{-19}$
20.69	$(5.53 \pm 0.31) \times 10^{-19}$	$(2.84 \pm 0.20) \times 10^{-19}$	$(3.92 \pm 0.28) \times 10^{-19}$
25.1	$(2.54 \pm 0.18) \times 10^{-19}$	$(1.45 \pm 0.08) \times 10^{-19}$	$(4.06 \pm 0.19) \times 10^{-19}$

The general shape of the ionization curves can be understood qualitatively by the following. At low-incident energies, i.e., small relative velocities, the cross section increases with energy because of the increased momentum transfer available to the electron of interest. At high energies, the cross section decreases with increasing energy because the interaction time between the projectile and target atoms is becoming appreciably smaller. The peak of the cross section occurs when the ion velocity and the velocity of the electron that is to be ionized are approximately equal.

B. Comparison with PWBA for ionization

Ionization cross sections have been computed utilizing the plane-wave Born approximation[12] (PWBA) for the one-electron ions of C, N, O, and F incident on He gas. The calculation utilizes the results of protons on hydrogen[14,17] scaled by the factor Z_1^2/Z_2^4, where Z_1 and Z_2 are the atomic numbers of the projectile and target atoms, respectively. The results of this calculation are compared to the experimentally determined cross sections for ionization in Fig. 3, where the curves represent the PWBA calculation for the various ions. As can be seen from the figure, the agreement between the experimental results and the PWBA calculation is excellent, within the limits of the experimental error. The close agreement between the two indicates that the PWBA calculation accurately describes the simple systems chosen for this experiment without the use of correction terms used in other studies.[18] Also, the comparison shows that the cross sections do indeed scale by the factor Z_1^2/Z_2^4, and the absolute magnitude of the curves for the various values of Z_2 are correct.

Other studies in the literature[18,19] utilize the PWBA in the range where $Z_1/Z_2 < 1$. In these works, a screening parameter θ_K is used to account for the departure from hydrogenlike wave functions. In this paper, screening parameters are not needed for the projectile since the incident ions are in pure hydrogenlike states. θ_k, in this case, equals one. Also included in these works are Coulomb-deflection, binding-energy, and polarization corrections (PWBABCP). These corrections, incorporated in an approximate manner, account for the deflection of the projectile by the target nucleus, and the perturbation, by the projectile, of the atomic states of the target atom. The contribution to the PWBA ionization cross sections by these correction terms, are shown in Fig. 4 for F^{8+} on helium. In general, the corrections due to Coulomb deflection are much less than 1%, while the binding-energy correction is significant. At low energies, the binding-energy correction lowers the cross section by about 40%, while at high energies, the cross section is lowered by approximately 10%. Thus, with the inclusion in the PWBA of the Coulomb-deflection and binding-energy corrections alone (PWBABC), the theoretical curves fall below the experimental data. If one also includes the polarization correction term in the PWBA, the theoretical curves are raised and once again fall within the experimental limits of the data. However, the present work shows that these corrections are not necessary in order to obtain

TABLE III. $O^{q+} \rightarrow He$; cross sections σ_{ij} in cm^2/atom with relative uncertainties.

Energy (MeV)	σ_{87}	σ_{76}	σ_{78}
9	$(3.51 \pm 0.26) \times 10^{-17}$	$(2.40 \pm 0.12) \times 10^{-17}$	$(1.25 \pm 0.13) \times 10^{-19}$
16	$(4.33 \pm 0.14) \times 10^{-18}$	$(2.48 \pm 0.07) \times 10^{-18}$	$(1.90 \pm 0.19) \times 10^{-19}$
20	$(1.63 \pm 0.10) \times 10^{-18}$	$(9.43 \pm 0.03) \times 10^{-19}$	$(2.36 \pm 0.21) \times 10^{-19}$
25	$(6.37 \pm 0.17) \times 10^{-19}$	$(3.82 \pm 0.24) \times 10^{-19}$	$(2.48 \pm 0.17) \times 10^{-19}$
30	$(2.89 \pm 0.15) \times 10^{-19}$	$(1.59 \pm 0.07) \times 10^{-19}$	$(2.07 \pm 0.18) \times 10^{-19}$
36	$(1.28 \pm 0.10) \times 10^{-19}$	$(7.57 \pm 0.46) \times 10^{-20}$	$(2.62 \pm 0.11) \times 10^{-19}$
40	$(8.56 \pm 1.02) \times 10^{-20}$	$(5.01 \pm 0.27) \times 10^{-20}$	$(2.49 \pm 0.08) \times 10^{-19}$

TABLE IV. $F^{q+} \rightarrow He$; cross sections σ_{ij} in cm^2/atom with relative uncertainties.

Energy (MeV)	σ_{98}	σ_{87}	σ_{89}
10.7	$(4.40 \pm 0.19) \times 10^{-17}$	$(3.48 \pm 0.11) \times 10^{-17}$	$(6.14 \pm 1.13) \times 10^{-20}$
13	$(2.24 \pm 0.09) \times 10^{-17}$	$(1.74 \pm 0.06) \times 10^{-17}$	$(5.90 \pm 1.08) \times 10^{-20}$
16	$(9.39 \pm 0.34) \times 10^{-18}$	$(7.73 \pm 0.36) \times 10^{-18}$	$(1.23 \pm 0.19) \times 10^{-19}$
19	$(5.26 \pm 0.23) \times 10^{-18}$	$(3.72 \pm 0.14) \times 10^{-18}$	$(1.07 \pm 0.13) \times 10^{-19}$
22	$(2.75 \pm 0.13) \times 10^{-18}$	$(1.98 \pm 0.22) \times 10^{-18}$	$(1.13 \pm 0.26) \times 10^{-19}$
25	$(1.75 \pm 0.06) \times 10^{-18}$	$(1.22 \pm 0.03) \times 10^{-18}$	$(1.08 \pm 0.10) \times 10^{-19}$
27	$(1.20 \pm 0.05) \times 10^{-18}$	$(8.23 \pm 0.25) \times 10^{-19}$	$(1.55 \pm 0.16) \times 10^{-19}$
29.7	$(8.99 \pm 0.56) \times 10^{-19}$	$(5.84 \pm 0.31) \times 10^{-19}$	$(1.58 \pm 0.10) \times 10^{-19}$
32	$(5.61 \pm 0.31) \times 10^{-19}$	$(4.04 \pm 0.09) \times 10^{-19}$	$(1.45 \pm 0.06) \times 10^{-19}$
35	$(3.50 \pm 0.31) \times 10^{-19}$		$(1.53 \pm 0.37) \times 10^{-19}$
41	$(2.24 \pm 0.19) \times 10^{-19}$	$(1.32 \pm 0.08) \times 10^{-19}$	$(1.55 \pm 0.21) \times 10^{-19}$
47	$(1.40 \pm 0.06) \times 10^{-19}$	$(8.28 \pm 0.59) \times 10^{-20}$	$(1.70 \pm 0.02) \times 10^{-19}$

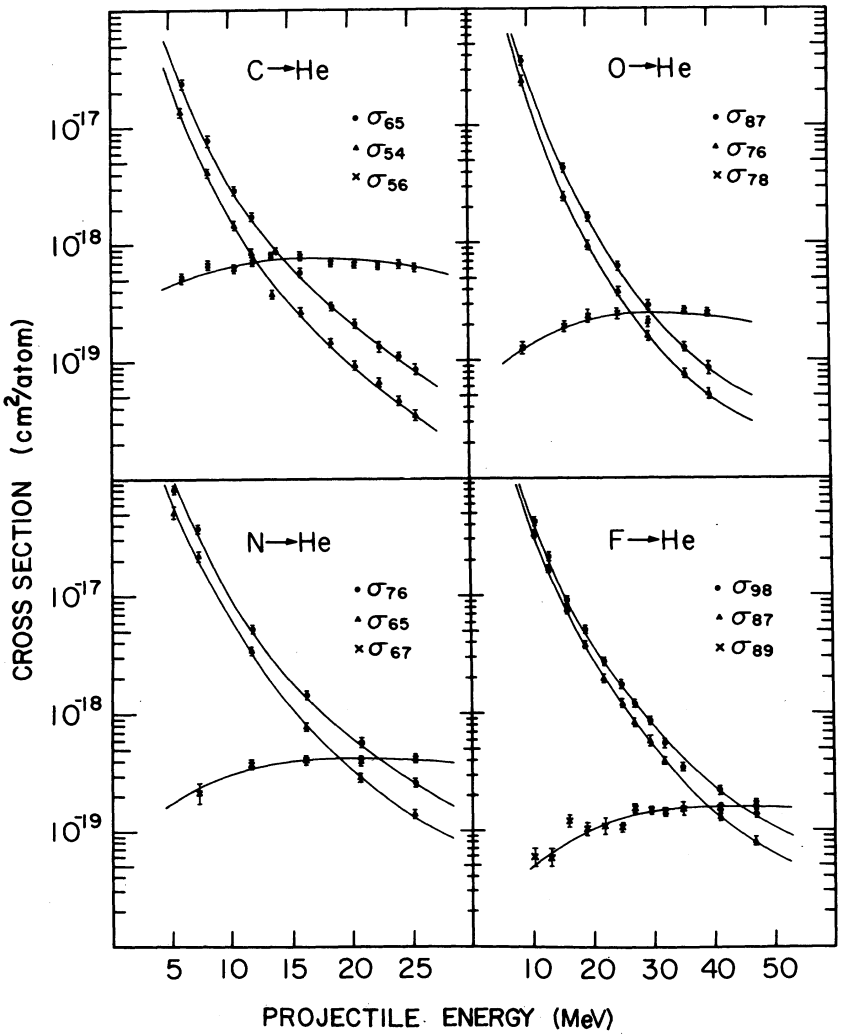

FIG. 2. Single-charge-transfer cross sections for the bare nuclei and one-electron ions of C, N, O, and F incident on He gas. The cross sections are given in units of cm^2/atom, as a function of projectile energy. The solid curves are drawn to guide the eye.

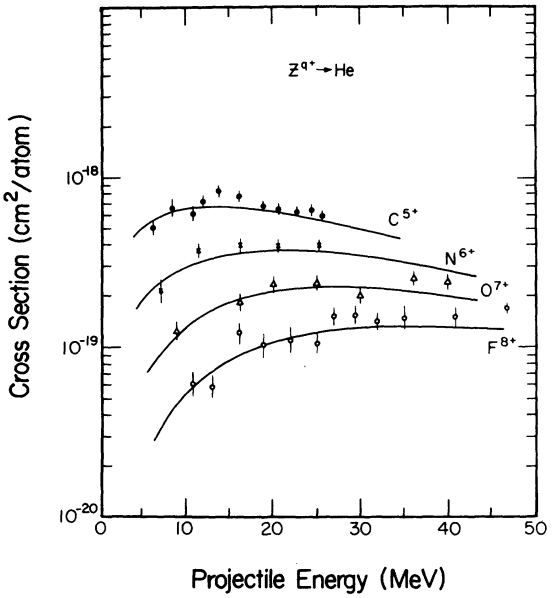

FIG. 3. Ionization cross sections for the one-electron ions of C, N, O, and F incident on He gas. The solid curves represent a theoretical PWBA calculation.

agreement between theory and experiment. The PWBA calculation, in which no correction terms are included, gives good agreement with experimental results. It should be noted, however, that the ionization process studied in this work is near the peak of the cross section where the PWBA and PWBABCP results are similar. Figure 4 shows

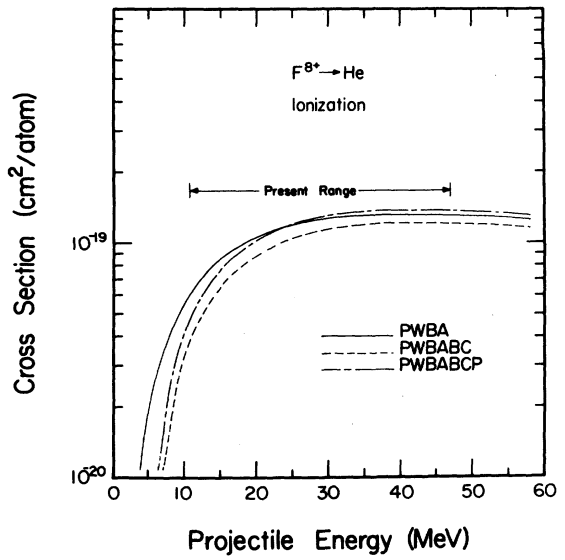

FIG. 4. Theoretical PWBA curves with Coulomb-deflection, binding-energy, and polarization corrections are shown for $F^{8+} \rightarrow He$. The cross sections are given over an extended energy range with the present range indicated by an arrow.

that these curves tend to diverge in the low-energy region. Thus measurements of the cross sections at lower energies for the one-electron ions would provide a good test for the corrections to the PWBA, but this remains a subject for further investigation.

C. Comparison with x-ray cross sections for electron capture

Following electron capture, x-ray production may result by a deexcitation process, if the capture was to an excited state of the atom. Figure 5 shows a comparison between the x-ray cross sections of Guffey,[16] and the capture cross sections of this work. The data are for the bare projectiles on helium and are given as a function of projectile energy. In general, at low energies the x-ray cross sections are approximately 70% of the capture cross sections. However, one sees that the x-ray cross sections fall more rapidly with energy than do the capture cross sections.

The x-ray and capture cross sections were also compared through the use of the function $g(Z_1, E)$ from Guffey,[16] where

$$g(Z_1, E) = \left(\frac{\sigma_{2p}}{\sigma_{TC}}\right)_{(Z_1, E)} + [1 - 0.12B(Z_1)] \sum_{n=3,l}^{n_{max}} \left(\frac{\sigma_{nl}}{\sigma_{TC}}\right)_{(Z_1, E)} . \quad (7)$$

The function essentially represents the fraction of capture events that gives rise to K x-rays and can be calculated if the capture cross section is known. The factor $0.12B(Z_1)$ represents the branching ratios for the states produced in capture to the Z_1 nucleus such that a K x ray occurs in the decay process. Guffey evaluated the capture cross sections, σ_{nl} through a Brinkman-Kramers (BK) formulation and related the results to the x-ray cross sections by means of

$$\sigma_x(Z_1, E) = \bar{N} g(Z_1, E) \sigma_{TC}(Z_1, E) , \quad (8)$$

where $\bar{N}$ is an overall normalization constant. The normalization constant was included since it is well known that the BK approximation leads to a large overestimation of the cross section. More recent theoretical work for other systems[20] have improved on the Oppenheimer-Brinkman-Kramers (OBK) approximation in giving the absolute cross section, but for capture of loosely bound electrons, such calculations have not been published. From the total capture cross sections found in this work, and the x-ray cross sections of Guffey, the value of $g(Z_1, E)$ was calculated and compared to the value found through the BK formulation. This comparison is shown in Fig. 6. It is clear from the

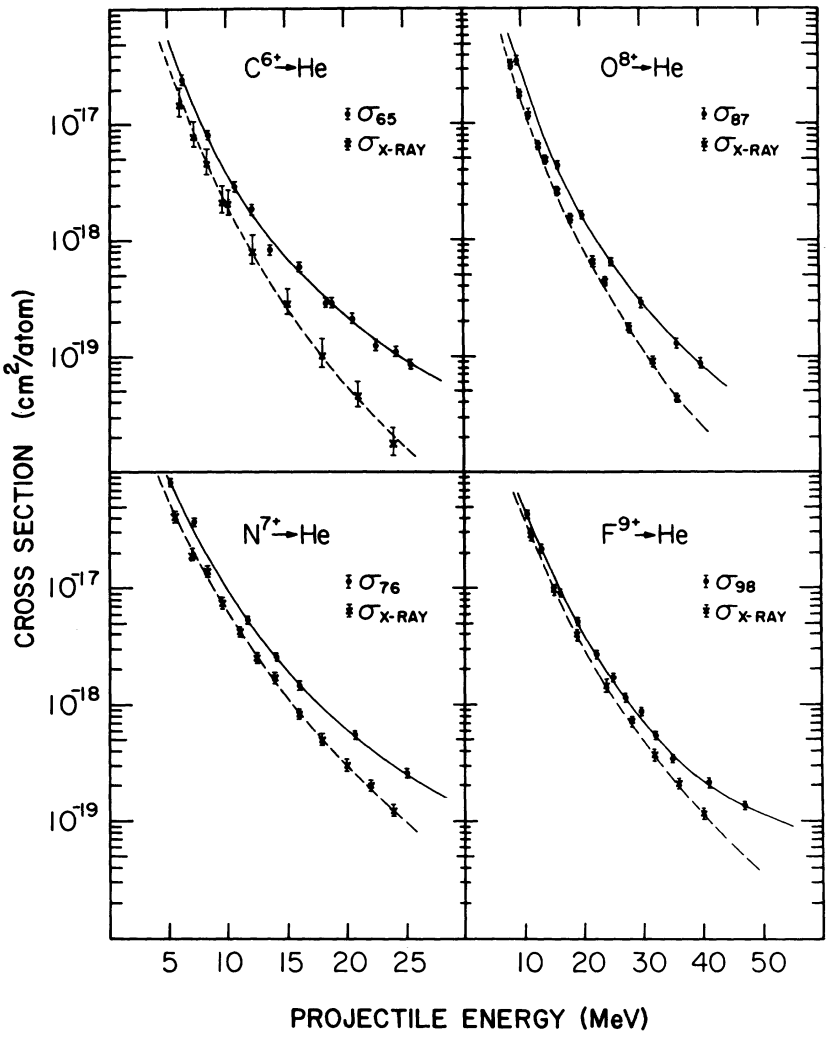

FIG. 5. A comparison between the single-electron-capture and x-ray cross sections for the bare nuclei of C, N, O, and F incident on He. The solid curves are drawn to guide the eye.

figure that the ratio of x-ray to capture cross sections obtained through a BK calculation does not agree with experimental results. This comparison shows that the single normalization constant for capture to each state, which was used in the theoretical analysis of the x-ray cross section, is inadequate. In particular, the present results show that the BK calculation underestimates the capture of the electron to the 1*s* and 2*s* states as compared to the higher, x-ray-emitting states.

Comparisons can also be made between the x-ray and capture cross sections for the one-electron projectiles incident on helium gas. This comparison is shown in Fig. 7. In this figure, there is an added feature in that the two curves cross over. This feature can be understood qualitatively in terms of the electron already present on the projectile. Not only can the capture of an electron by the projectile give rise to K x rays, but also the excitation of the electron already present on the projectile can contribute to the total x-ray cross section. The latter contribution increases rapidly with increasing energy towards a maximum which occurs when the velocity of the projectile and the mean velocity of the K-shell electron are approximately equal. Hence, the single-electron-capture and total x-ray curves cross over for the one-electron projectiles.

D. q dependence for electron capture

The total capture cross sections are also plotted in Fig. 8 as a function of E/M (MeV/amu). It is evident that the data fall on three curves which can be associated with the charge-changing processes $q \rightarrow q-1$ for $q=8$, 7, and 6. Thus, for a given velocity the capture depends only on the

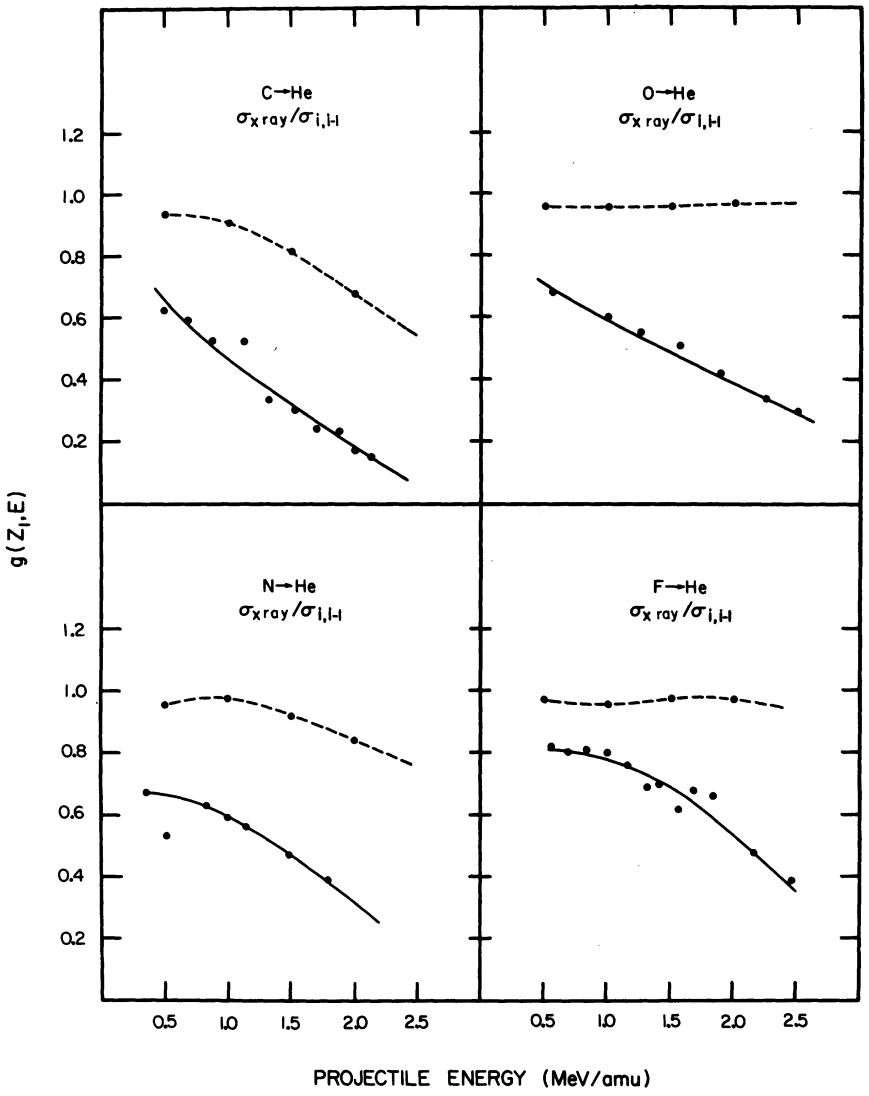

FIG. 6. The function $g(Z_1, E)$ calculated from a Brinkman-Kramers formulation (dashed lines) as compared to the same function found utilizing the capture cross sections of this work (solid lines).

charge state of the ion. For example, F^{8+} and O^{8+} have the same capture cross section at the same E/M value. In addition, the three curves have similar velocity dependences with average ratios of 1:0.68:0.44 for the 8-7, 7-6, and 6-5 cross sections, respectively. These ratios are consistent with a q^3 dependence of the total cross section.[21] The q^3 dependence predicts ratios of 1:0.67:0.42 for the 8-7:7-6:6-5 cross sections.

The data presented here are also in good agreement with the "simple theoretical estimates" of Knudsen *et al.*[22] for the capture cross section based on the model of Bohr and Lindhard.[23] Knudsen *et al.* present the capture cross section in terms of a universal curve which has a different character in energy regions referred to as low, medium and high energy. The present data fall in the high-energy region where the capture cross section follows a q^3 dependence similar to that presented in the previous paragraph, but is plotted on their universal curve as σ_c/q vs $E/q^{4/7}$.

V. SUMMARY

Single-electron-capture and electron-loss cross sections have been experimentally measured for bare nuclei and one-electron ions of carbon, nitrogen, oxygen, and fluorine incident on helium gas. The cross sections were measured as a function of energy in the range of ~0.5–2.5 MeV/amu. Low-target gas pressures were utilized to extract charge-transfer cross sections by the initial

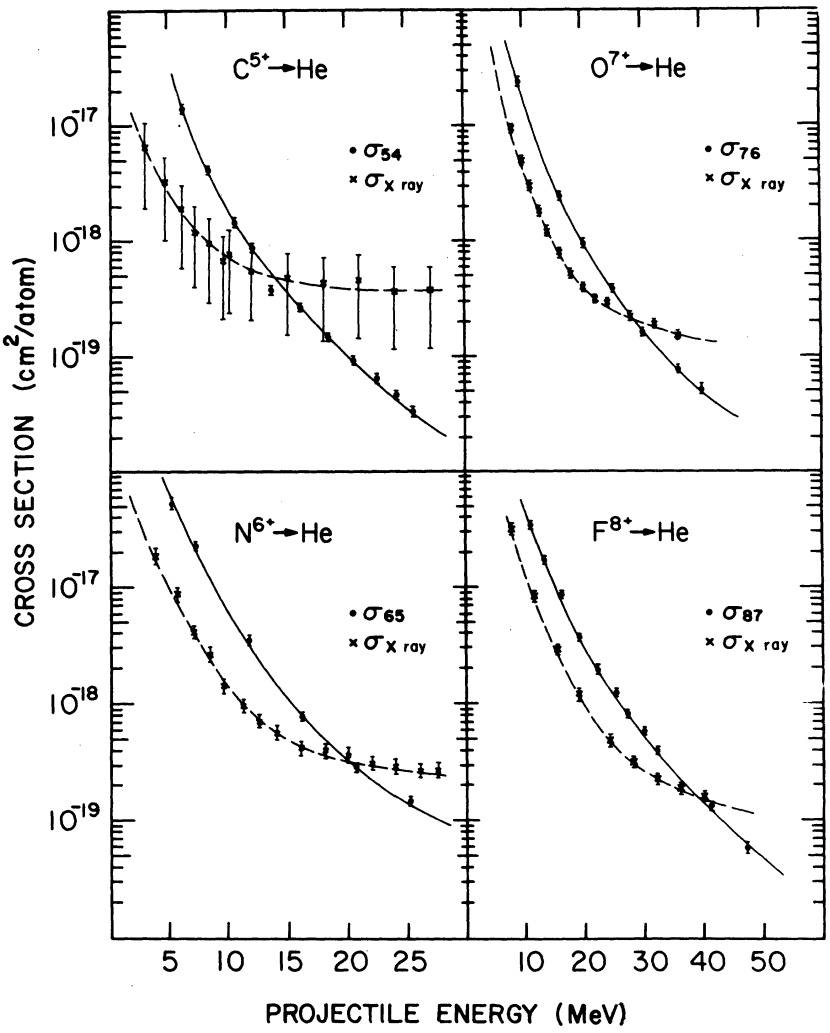

FIG. 7. A comparison between the single-electron-capture and x-ray cross sections for the one-electron ions of C, N, O, and F incident on He. The solid curves are drawn to guide the eye.

growth method. In general, single-capture cross sections fall off by several orders of magnitude with increasing projectile energy. The ionization cross sections, however, exhibit a very broad maximum over the range of interest.

Comparisons have been made between the ionization cross sections for the various ions and a theoretical PWBA calculation. The PWBA calculation utilizes the results of protons on hydrogen scaled by the factor Z_1^2/Z_2^4. For the hydrogenlike ions used, the agreement between the experimental results and the theoretical calculation is remarkably good. The PWBA cross sections are lowered by approximately 40% at low energies, and 10% at high energies by including Coulomb-deflection and binding-energy corrections in the calculation. Hence, the PWBABC does not give good agreement with the experimental results. With the additional correction from polarization, the agreement is once again good. However, the present results show that these corrections are not necessary in order to obtain agreement between experiment and theory since the PWBA calculation, without the inclusion of any correction terms, gives good agreement.

Single-electron-capture cross sections were compared to total x-ray cross sections. The results of this comparison confirm the magnitude of the x-ray cross sections to an accuracy of ~30%. A comparison was also made for the ratio of the x-ray cross section to the total capture cross section from this work, to the same ratio calculated from a Brinkman-Kramers formulation. The agreement between experiment and the BK

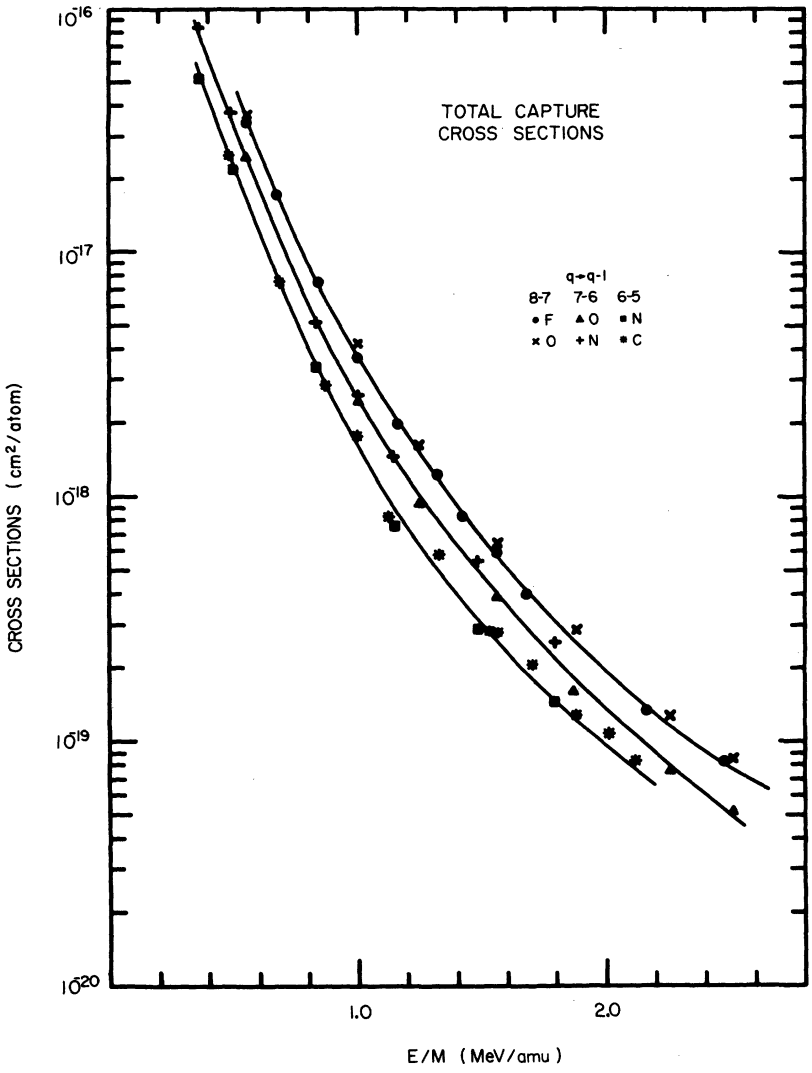

FIG. 8. Single-electron-capture cross sections associated with the charge-changing process $q \rightarrow q-1$ for $q=8$, 7, and 6 as a function of E/M (MeV/amu). The solid curves are drawn to guide the eye.

calculation is poor. This shows that the single normalization constant used in the analysis of the x-ray cross sections for capture to each state is inadequate. In particular, the capture of the electron to the 1*s* and 2*s* states is underestimated, as compared to the higher x-ray-emitting states, in the BK calculation. The total capture cross sections were also plotted as a function of E/M (MeV/amu). The results show that the capture is dependent only upon the velocity and the charge state of the incident ion. Also, the similar velocity dependence for the charge-changing process $q \rightarrow q-1$ ($q=8$, 7, and 6) corresponds to a q^3 dependence for the total cross section.

ACKNOWLEDGMENTS

The authors would like to thank J. H. McGuire for his assistance with the theoretical calculations and many helpful discussions on the subject of this work. This work was supported by the Division of Chemical Sciences, U. S. Department of Energy.

*Deceased, December, 1979.
[1]P. Richard, in *Atomic Inner-Shell Processes*, edited by B. Crasemann (Academic, New York, 1975), Vol. I, pp. 74–152.
[2]C. F. Barnett, *The Physics of Electronic and Atomic Collisions*, Invited Lectures, Review Papers and Progress Reports of the Ninth International Conference on the Physics of Electronic and Atomic Collisions, Seattle, 1975, edited by J. S. Risley and R. Geballe, (University of Washington, Seattle, 1975), pp. 846–853.
[3]G. Steigman, Astrophys. J. 199, 642 (1975).
[4]M. R. C. McDowell and J. P. Coleman, *Introduction to the Theory of Ion-Atom Collisions* (North-Holland, Amsterdam, 1970), Chap. 7.
[5]J. R. Macdonald and F. W. Martin, Phys. Rev. A 4, 1965 (1971).
[6]T. Chiao, Ph.D. thesis, Kansas State University, 1973 (unpublished).
[7]S. K. Allison and M. Garcia-Munoz, in *Atomic and Molecular Processes*, edited by D. R. Bates (Academic, New York, 1962), pp. 721–782.
[8]V. S. Nikolaev, Usp. Fiz. Nauk 85, 679 (1965) [Sov. Phys.—Usp. 8, 269 (1965)].
[9]H. D. Betz, Rev. Mod. Phys. 44, 465 (1972).
[10]H. Tawara and A. Russek, Rev. Mod. Phys. 45, 178 (1973).
[11]J. D. Garcia, R. J. Fortner, and T. M. Kavanagh, Rev. Mod. Phys. 45, 111 (1973).
[12]E. Merzbacher and H. W. Lewis, in *Encyclopedia of Physics*, edited by S. Flügge (Springer, Berlin, 1958), Vol. 34, p. 166.
[13]H. Tawara, P. Richard, K. A. Jamison, Tom J. Gray, J. Newcomb, and C. Schmiedekamp, Phys. Rev. A 19, 1960 (1979); H. Tawara, P. Richard, K. A. Jamison, and Tom J. Gray, J. Phys. B 11, L615 (1978); H. Tawara, M. Terasawa, P. Richard, T. J. Gray, P. Pepmiller, J. Hall, and J. Newcomb, Phys. Rev. A 20, 2340 (1979).
[14]J. H. McGuire (private communication).
[15]G. Basbas, in *Electronic and Atomic Collisions*, edited by J. S. Risley and R. Geballe (University of Washington Press, Seattle, 1975), p. 502.
[16]J. A. Guffey, Ph.D. thesis, Kansas State University, 1976 (unpublished); J. A. Guffey, L. D. Ellsworth, and J. R. Macdonald, Phys. Rev. A 15, 1863 (1977).
[17]J. Golden, Ph.D. thesis, Kansas State University, 1975 (unpublished).
[18]G. Basbas, W. Brandt, and R. Laubert, Phys. Rev. A 7, 983 (1973); 17, 1655 (1978).
[19]G. S. Khandelwal, B. H. Choi, and E. Merzbacher, At. Data 1, 103 (1969).
[20]A. M. Halpern and J. Law, Phys. Rev. A 12, 1776 (1975); K. Omidvar, J. E. Golden, and J. H. McGuire, *ibid.* 13, 500 (1976); C. D. Lin, S. C. Soong, and L. N. Tunnell, *ibid.* 17, 1646 (1978); Dz. Belkic, R. Gayet, and A. Salin, Phys. Rep. 56, 281 (1979); J. Eichler and F. T. Chan, Phys. Rev. A 20, 104 (1979).
[21]H. Tawara, Phys. Lett. 71A, 208 (1979).
[22]H. Knudsen, H. K. Haugen, and P. Hvelplund, Phys. Rev. A 23, 597 (1981).
[23]N. Bohr and J. Lindhard, K. Dan. Vidensk. Selsk. Mat. Fys. Medd. 28, No. 7 (1954).